

NeurBench: Benchmarking Learned Database Components with Data and Workload Drift Modeling

Zhanhao Zhao¹, Haotian Gao¹, Naili Xing¹, Lingze Zeng¹, Meihui Zhang²,
Gang Chen³, Manuel Rigger¹, Beng Chin Ooi¹

¹ National University of Singapore ² Beijing Institute of Technology ³ Zhejiang University
{zhzhao, gaohaotian, xingnl, lingze, rigger, ooibc}@comp.nus.edu.sg meihui_zhang@bit.edu.cn cg@zju.edu.cn

ABSTRACT

Learned database components, which deeply integrate machine learning into their design, have been extensively studied in recent years. Given the dynamism of databases, where data and workloads continuously drift, it is crucial for learned database components to remain effective and efficient in the face of data and workload drift. Adaptability, therefore, is a key factor in assessing their practical applicability. However, existing benchmarks for learned database components either overlook or oversimplify the treatment of data and workload drift, failing to evaluate learned database components across a broad range of drift scenarios. This paper presents NeurBench, a new benchmark suite that applies measurable and controllable data and workload drift to enable systematic performance evaluations of learned database components. We quantify diverse types of drift by introducing a key concept called the drift factor. Building on this formulation, we propose a drift-aware data and workload generation framework that effectively simulates real-world drift while preserving inherent correlations. We employ NeurBench to evaluate state-of-the-art learned query optimizers, learned indexes, and learned concurrency control within a consistent experimental process, providing insights into their performance under diverse data and workload drift scenarios.

1 INTRODUCTION

Database systems are increasingly embracing machine learning (ML) techniques in their design. Key database components, such as query optimizers, indexes, and concurrency control (CC), are being upgraded with ML models to boost performance. For example, learned query optimizers [39, 66] treat query optimization as an ML problem to obtain more efficient query plans. Learned indexes [13, 23] replace traditional index structures with ML models that predict the positions of query keys, enabling faster key search. Similarly, learned CC algorithms [53] predict optimal CC actions (e.g., locking strategies and blocking timeouts) for different operations to improve transaction throughput.

One major challenge faced by learned database components is the dynamic nature of databases, commonly referred to as *data and workload drift* [24, 25, 61]. Specifically, the data stored in databases constantly changes over time due to inserts, updates, and deletions, while workloads also evolve, with drift in query patterns [17] and query/transaction arrival rates [34]. In contrast, ML models typically derive insights from static datasets, and this fundamental difference between the paradigms of databases and ML can cause learned database components to be ineffective and outdated in the face of data and workload drift. For instance, as data is updated over time, learned query optimizers may lose precision because

the knowledge they initially learned for generating query plans becomes obsolete. Similarly, learned CC algorithms may choose actions that were once optimal but no longer suit the current workload with drifted transaction arrival rates.

Achieving adaptive learned database components that remain effective regarding data and workload drift is crucial. Early approaches [23, 40, 51] typically overlook the adaptability issue or suggest that it can only be addressed through complete model retraining. Consequently, when models become outdated, costly manual intervention and retraining are necessary, making them inefficient in dealing with continuous data and workload drift. More recently, improving adaptability has been gaining significant attention in our community. For example, specific mechanisms [25, 31, 61, 64] are proposed to automatically detect drift and trigger model retraining or fine-tuning for learned database components. Moreover, recent research [52] utilizes advanced deep neural networks with inherently stronger generalizability to build more robust learned database components [32]. In tandem with the advancement of ML techniques, we envision continued efforts to enhance the adaptability of learned database components.

The rapid developments in adaptive learned database components naturally raise a pertinent question: how well do existing learned database components perform under data and workload drift, and how do their key designs impact performance under different drift scenarios? To be able to answer this question meaningfully, we need comprehensive empirical evaluations and benchmarks that assess learned database components in the context of various data and workload drift. Thus far, several efforts have been made to evaluate representative learned database components, such as learned query optimizers [12, 18, 24, 27] and learned indexes [48, 59]. However, their treatment of data and workload drift is rather simplistic and arbitrary. For example, data drift is simulated by directly deleting half of a table [24, 27], while workload drift is modeled by randomly sampling queries from a predefined query set [61]. In particular, there are two major limitations: 1) They lack *effective control* over data and workload drift. Given that real-world drift occurs continuously and incurs various drift scenarios, this drawback prevents in-depth evaluation of learned database components under varying degrees of drift, and makes it challenging to identify the exact threshold at which these components fail to remain effective. 2) Their drift simulations typically overlook the *inherent correlations* in real-world data and workloads. For example, in an e-commerce database, attributes such as user demographics (e.g., age, location) are often correlated with purchasing behavior (e.g., product category, spending patterns). Evaluations under unrealistic drift scenarios may not accurately reflect the components' performance in practical applications.

To address these limitations, we design a comprehensive benchmark suite that can simulate real-world data and workload drift, thereby enabling in-depth evaluations of different learned database components under diverse drift scenarios. Accordingly, we have to fulfill two key requirements. First, it is essential to uniformly and effectively quantify data and workload drift. However, given the various drift in databases, such as data drift, query pattern drift, *etc.*, consistently defining and measuring all drift scenarios is non-trivial. Second, real-world data and workloads exhibit intricate relationships among the attributes, and therefore, introducing specific drift while preserving these correlations is challenging. The drift simulation must effectively capture inherent correlations to ensure that the drifted data and workloads remain representative of real-world scenarios.

In this paper, we present NeurBench, a novel benchmark suite designed to evaluate various learned database components under controllable data and workload drift. Unlike existing benchmarks, NeurBench standardizes the evaluation process by introducing systematic drift factor modeling. In particular, we define a concept called the *drift factor* to quantify data and workload drift in a unified manner. We model all types of drift as changes in underlying probabilistic distributions and measure drift as the distance between these distributions. Leveraging this concept, NeurBench generates data or workloads that exhibit a specified degree of drift from the original, offering fine-grained control over drift intensity. We then utilize the generated and original data and workloads to construct meaningful drift scenarios, ensuring comparable evaluations across diverse learned database components.

We propose a drift-aware data and workload generation framework capable of introducing specific drift to the original data and workloads while preserving their inherent correlation. Specifically, we first utilize a base generative model to learn the underlying distribution of the real data and workloads, and then train an independent *drifter* module to guide the base model in generating drifted data and workloads. The base generative model is built on the Denoising Diffusion Probabilistic Model (DDPM) [19]. Based on the proposed drift factor, we ensure the drifter effectively controls the generation process to introduce targeted drift while maintaining feature correlations. By decoupling the drifter from the base model, our framework generalizes across various types of drift, eliminating the need to train a specialized model for each drift scenario.

In summary, we make the following contributions:

- We introduce NeurBench, a practical benchmark suite that facilitates the evaluation of learned database components under controllable data and workload drift.
- We propose a unified concept called the drift factor to model data and workload drift, enabling the systematic performance evaluation of database components under diverse drift scenarios.
- We propose a drift-aware data and workload generation framework that effectively synthesizes drifted data and workloads according to a specified drift factor while preserving their inherent correlations.
- We conduct extensive experiments to demonstrate the effectiveness of NeurBench in generating drifted data and workload, and use NeurBench to evaluate start-of-the-art learned query optimizers, learned indexes, and learned CC. We report general

trends for these learned database components *w.r.t* diverse data and workload drift, and based on the results, we effectively identify the performance trade-off of different design choices under specific drift scenarios.

The remainder of the paper is structured as follows. Section 2 provides relevant background. Section 3 describes the overall design of NeurBench. Section 4 formally defines the drift factor and presents the drift-aware data and workload generation framework in detail. Section 5 describes the benchmarking preparation. Section 6 shows the experimental results. Section 7 discusses the related work, and Section 8 concludes.

2 BACKGROUND

In this section, we provide the necessary background of learned database components, drift in databases, and diffusion models.

2.1 Learned Database Components

Our study aims to be sufficiently general to systematically benchmark various learned database components, such as learned query optimizers, learned indexes, *etc.* Since these components typically rely on ML models, we provide a general definition of learned database components by mapping them to learnable ML functions:

Definition 1 (Learned Database Component). Consider a database that stores data \mathbf{R} and handles workload \mathbf{Q} . A learned database component can be formulated as an ML function $f(\cdot; \theta) : \mathbf{Z} \rightarrow \mathbf{Y}$, where θ denotes the trainable parameters. The input space \mathbf{Z} consists of features derived from the data \mathbf{R} and workload \mathbf{Q} , such as data distributions and query patterns. The output space \mathbf{Y} represents the predictions or decisions, such as estimated query plans, index positions, or concurrency control actions. The parameters θ are trained by a stochastic learning algorithm \mathcal{A} (e.g., Stochastic Gradient Descent), which adjusts θ to minimize a loss function $\mathcal{L}(f(\mathbf{Z}; \theta), \mathbf{Y})$ representing the discrepancy between the predicted output and the ground truth. The learning process can be formally expressed as:

$$\theta = \mathcal{A}(\mathbf{Z}, \theta^r, \mathcal{L}),$$

where θ^r represents the initial random weights of the model, and \mathcal{A} iteratively updates θ based on the gradients computed *w.r.t.* the loss function \mathcal{L} .

A learned database component may continuously refine its model parameters θ based on feedback from actual query execution and data/workload drift, ensuring its output \mathbf{Y} meets the following performance objective:

Definition 2 (Performance Objective). An optimal learned database component is expected to maximize system performance (e.g., minimizing latency, execution cost, or resource consumption) over a time window $\mathbf{T} = (ts_1, ts_2, \dots, ts_N)^\top$. Let $\psi(\mathbf{R}^{(i)}, \mathbf{Q}^{(i)})$ denote the performance metric at time ts_i , where $\mathbf{R}^{(i)}$ and $\mathbf{Q}^{(i)}$ are the data and workload at time ts_i , respectively, the performance objective is then to find optimal model parameters θ^* , such that

$$\theta^* = \arg \max_{\theta} \mathbb{E}_{ts_i \in \mathbf{T}} [\psi(\mathbf{R}^{(i)}, \mathbf{Q}^{(i)})],$$

where $\mathbb{E}[\cdot]$ denotes the expected performance.

2.2 Data and Workload Drift

Data stored in databases, as well as the workloads they handle, are subject to continuous drift. *Data drift* occurs due to operations including inserts, updates, deletes, and schema modifications. *Workload drift* refers to variations in the queries and transactions processed by the database over time, which can be further categorized into 1) Query pattern drift: changes in query structure, such as join patterns (FROM clauses) and predicate conditions (WHERE clauses); 2) Arrival rate drift: fluctuations in the volume and concurrency of queries and transactions.

Intuitively, data and workload drift naturally occur over time in databases. In addition, ML models are typically trained on fixed datasets, and their performance can degrade significantly when tested on data that deviate from the training distribution, *i.e.*, an issue commonly known as the distribution drift or out-of-distribution problem [21, 58]. As a result, to evaluate learned database components under drift scenarios, we model drift as temporal changes in data and workload distributions, ensuring a unified formulation that captures both data drift and workload drift. Drift may occur in the data, the workload, or both, depending on whether the distribution of \mathbf{R} , \mathbf{Q} , or their joint distribution changes over time:

Definition 3 (Data and Workload Drift). Consider a database operates over a time window \mathbf{T} consisting of N time slots, *i.e.*, $\mathbf{T} = (ts_1, ts_2, \dots, ts_N)^\top$, where $N \geq 2$. Let $\mathbf{R}^{(i)}$ and $\mathbf{Q}^{(i)}$ be random variables representing the state of the data and the workload, respectively, at time ts_i . Data and workload drift occurs when the distributions of data \mathbf{R} and workload \mathbf{Q} exhibit temporal changes across the time window \mathbf{T} . Let $\mathbb{P}_{\mathbf{R}^{(i)}, \mathbf{Q}^{(i)}}(\mathbf{r}, \mathbf{q})$ represent the joint probability density function of data \mathbf{R} and workload \mathbf{Q} at time ts_i . Drift happens if, for any two timestamps $i, j \in N$, where $i \neq j$,

$$\mathbb{P}_{\mathbf{R}^{(i)}, \mathbf{Q}^{(i)}}(\mathbf{r}, \mathbf{q}) \neq \mathbb{P}_{\mathbf{R}^{(j)}, \mathbf{Q}^{(j)}}(\mathbf{r}, \mathbf{q}).$$

Constructing realistic data and workload drift scenarios that capture meaningful distribution drift is crucial for evaluating the adaptability of learned database components. We note that there are existing benchmarks [15, 21] that enable the evaluation of ML models under distribution drift. However, they typically construct the drift scenario by collecting real-world data exhibiting distribution drift, which incurs two major limitations: First, they typically focus on data drift while overlooking workload drift, making them inadequate in benchmarking learned database components under various types of drift in both data and workloads. Second, relying on real-world data collection constrains the scope of drift scenarios that can be tested, as it can only cover observed drift patterns. To overcome these limitations, we opt to synthesize drifted data and workload while maintaining realism. Specifically, we learn the underlying distributions and their drift from real data and workloads, and propose a generation framework that enables the controlled synthesis of drifted data and workloads, thus ensuring comprehensive evaluations of learned database components under various degrees and types of drift.

2.3 Denoising Diffusion Probabilistic Model

Diffusion models, *e.g.*, Denoising Diffusion Probabilistic Models (DDPMs) [19], are powerful generative models that have been recently adopted to synthesize high-quality data, such as images [11],

audio [35], and tabular data [22, 36]. Inspired by the physical process of diffusion, where information (*e.g.*, particles, data) is gradually dispersed over time, these models learn to reverse this process so that a target distribution can be generated from a given prior distribution (Gaussian distribution as in DDPM) by a series of Markov transitions. In particular, diffusion models operate in two key stages, *i.e.*, forward process and reverse process, with slight variations in the details depending on the specific model. For illustration purposes, we use DDPM as a representative to formally explain these stages: **Diffusion (Forward) Process.** This process incrementally corrupts the data by adding Gaussian noise in discrete timesteps, ultimately transforming it into a simple noise distribution. Given a data sample $\mathbf{x}_0 \sim q(\mathbf{x})$ from the true data distribution $q(\mathbf{x})$, the forward process is formulated as a Markov chain:

$$q(\mathbf{x}_t | \mathbf{x}_{t-1}) = \mathcal{N}(\mathbf{x}_t; \sqrt{1 - \beta_t} \mathbf{x}_{t-1}, \beta_t \mathbf{I}),$$

where β_t represents the variance schedule controlling the noise added at each step t . The data distribution after T timesteps, $q(\mathbf{x}_T)$, approximates an isotropic Gaussian distribution $\mathcal{N}(\mathbf{0}, \mathbf{I})$.

Denosing (Reverse) Process. This process reconstructs the target data \mathbf{x}_0 by iteratively denoising \mathbf{x}_t in reverse timesteps, starting from $\mathbf{x}_T \sim \mathcal{N}(\mathbf{0}, \mathbf{I})$. The reverse process $p(\mathbf{x}_{t-1} | \mathbf{x}_t)$ can be approximated as a Gaussian distribution:

$$p(\mathbf{x}_{t-1} | \mathbf{x}_t) = \mathcal{N}(\mathbf{x}_{t-1}; \boldsymbol{\mu}(\mathbf{x}_t, t; \theta), \sigma_t^2 \mathbf{I}),$$

where $\boldsymbol{\mu}$ is learned parameters that estimate the mean of the reverse process, while σ_t^2 is derived from β_t .

Guided Diffusion. The reverse process can incorporate auxiliary information c , yielding a conditional reverse process $p(\mathbf{x}_{t-1} | \mathbf{x}_t, c)$, where the conditioning variable c may represent factors such as correlation-preserving constraints, or contextual information [11, 36]. By applying the Bayes' theorem, $p(\mathbf{x}_{t-1} | \mathbf{x}_t, c)$ can be decomposed as:

$$p(\mathbf{x}_{t-1} | \mathbf{x}_t, c) \propto p(\mathbf{x}_{t-1} | \mathbf{x}_t) \Pr(c | \mathbf{x}_{t-1}, \mathbf{x}_t).$$

In particular, $p(\mathbf{x}_{t-1} | \mathbf{x}_t)$ should perform unconditional generation, while $\Pr(c | \mathbf{x}_{t-1}, \mathbf{x}_t)$ guides the reverse process to introduce the specified condition c . Inspired by such guided diffusion models, we treat the introduction of drift to data and workloads as a specific condition, and propose a novel drift-aware data and workload generation framework based on diffusion models.

3 OVERVIEW OF NeurBench

In this section, we introduce the system overview of NeurBench, as shown in Figure 1. To systematically evaluate learned database components under controllable data and workload drift, we design NeurBench with two key modules, a *drift-aware data and workload generator*, and a *performance evaluator*. After receiving the original data and workloads from users, the generator synthesizes drifted data and workloads, which are combined with the original ones as the drift scenarios so that the evaluator can then utilize it to conduct evaluations. We now provide more details on the generator and the evaluator, respectively.

Drift-aware Data and Workload Generator. We allow users to specify the desired drift level using a *drift factor* d , where $d \in [0, 1]$. By default, users can independently indicate drift factors for either data or workload to achieve effective control over each. A drift

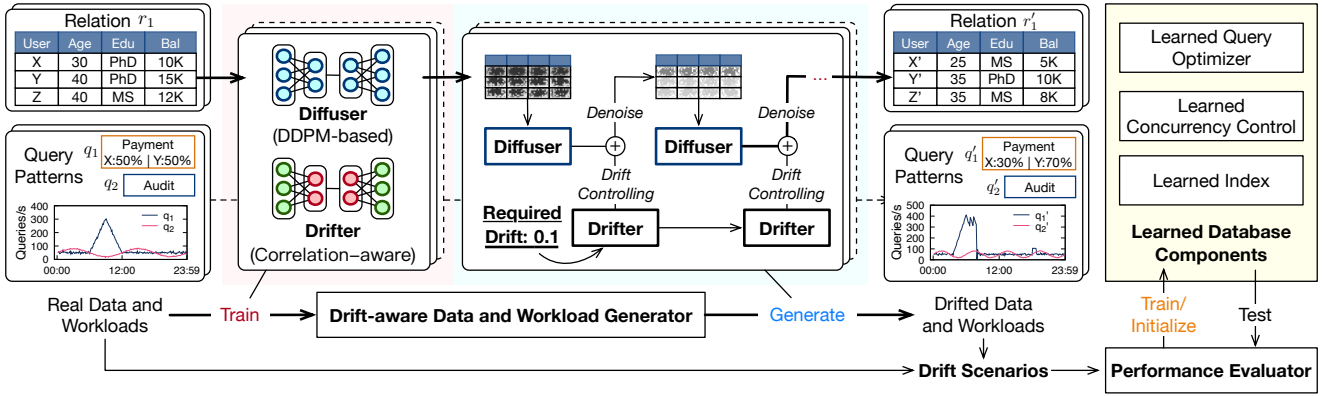


Figure 1: System Overview of NeurBench

factor of $d=0$ indicates no drift, while $d=1$ denotes that the entire data or workload is fully drifted. Section 4.1 provides the formal definition of the drift factor.

Given a specified drift factor d as input, the idea is to drift the given original data (workload) to a target data (workload) that aligns with d , thereby enabling controllable drifted data and workload generation. In addition, we capture real-world drift patterns to ensure that the generated data and workloads exhibit realistic drift behaviors. To achieve this, we design the *generator* based on guided diffusion, which consists of two components: 1) *Diffuser*, a DDPM-based generative model that learns the underlying distribution of the original data and workloads; 2) *Drifter*, a drift-controlling module that guides the diffuser to yield a conditional denoising process. To synthesize drifted data and workloads, starting from a standard normal distribution, we iteratively invoke the diffuser to denoise the distribution, while leveraging the drifter to introduce drift at each denoising step, gradually transforming the distribution into the target distribution. Moreover, the drifter is explicitly trained to introduce drift patterns that align with real-world scenarios while preserving the inherent correlations within the data and workloads. Section 4.2 details the diffuser and drifter construction.

Performance Evaluator. To effectively assess the adaptability and robustness of learned database components, we evaluate their performance across various drift scenarios. Given a drift factor d , we use the generator to synthesize drifted data and workloads based on d . We impose no constraints on drift scenario construction, and allow users to flexibly construct drift scenarios by selecting whether to use drifted or original data/workloads for training and testing. By default, we train or initialize learned database components using drifted data and workloads generated based on a specific d , and evaluate them on a fixed test set sampled from the original data and workloads. After repeating this process with different drift factors, we can construct several drift scenarios and ensure the comparability of results across varying drift scenarios.

Running Example. We now provide a running example to demonstrate the use of NeurBench in generating drifted data and workloads with a specified drift factor $d=0.1$. For data, let us consider an original user table r_1 with attributes including user name, age, education level (Edu), and balance (Bal). As shown in Figure 1, we train a diffuser and a drifter for r_1 . The diffuser learns the underlying data distribution, and therefore, it captures the inherent correlations,

such as the tendency of older users with higher education levels to have larger account balances. Further, the drifter introduces certain drift while preserving correlations, e.g., as the average age slightly decreases, the education level distribution drifts accordingly, and balances are reduced overall. We then provide the drift factor d to the drifter, allowing precise control over the intensity of the drift introduced. Guided by the drifter, the diffuser generates the drifted table r_1' , ensuring that the original correlations are preserved while aligning with the specified drift factor. For the workload generation, we model the workload as a set of query patterns, such as q_1 for payment processing and q_2 for auditing, each following specific arrival rates, as shown in Figure 1. We then train a specialized diffuser and drifter to synthesize the workload with drifted queries and corresponding arrival rates. For instance, after applying drift, q_1 may change its focus to 30% of user X and 70% of user Y, indicating an increased demand for auditing processes.

Without loss of generality, we take an example of evaluating learned query optimizers under data drift with two different drift factors. We use the generator to derive two drifted tables from r_1 , namely r_1' and r_1'' , each corresponding to a specified drift factor. The learned query optimizer is then trained separately on r_1' and r_1'' and evaluated using a consistent test set derived from the original table r_1 to ensure fair and comparable performance evaluations.

4 CONTROLLED DRIFT GENERATION

In this section, we formalize the drift factor and introduce the drift-aware data and workload generation framework in detail.

4.1 Drift Factor Modeling

We aim to define a drift factor that can uniformly and effectively describe the differences in data and workloads over time, thus facilitating the generation of new data or workloads from initial ones with specific drift. In our problem setting, the drift factor must satisfy two key properties: 1) It should accurately capture the differences between data or workloads while providing a bounded value range for users to specify the desired drift. 2) Its value should provide a consistent representation for all types of drift.

According to Definition 3, where drift is mapped to the underlying distribution of data and workloads, we define the drift factor based on the distance of distributions. To satisfy the properties

above, we utilize the *Jensen-Shannon (JS) divergence* [38]. Specifically, given a distribution \mathbb{P} and the drifted one \mathbb{P}' , their JS divergence $\mathcal{D}_{JS}(\mathbb{P} \parallel \mathbb{P}')$ is defined as:

$$\mathcal{D}_{JS}(\mathbb{P} \parallel \mathbb{P}') = \frac{1}{2} \mathcal{D}_{KL}(\mathbb{P} \parallel \mathbb{M}) + \frac{1}{2} \mathcal{D}_{KL}(\mathbb{P}' \parallel \mathbb{M}),$$

where $\mathbb{M} = \frac{1}{2}(\mathbb{P} + \mathbb{P}')$, and \mathcal{D}_{KL} is the Kullback–Leibler (KL) divergence, which is defined by:

$$\mathcal{D}_{KL}(\mathbb{P} \parallel \mathbb{P}') = \sum_x \mathbb{P}(x) \log \frac{\mathbb{P}(x)}{\mathbb{P}'(x)}.$$

\mathcal{D}_{JS} satisfies $\mathcal{D}_{JS}(\mathbb{P} \parallel \mathbb{P}') = \mathcal{D}_{JS}(\mathbb{P}' \parallel \mathbb{P})$, and is bounded within $[0, \log 2]$. Normalizing it by $\log 2$, the drift factor d is defined as:

$$d(\mathbb{P}, \mathbb{P}') = \frac{\mathcal{D}_{JS}(\mathbb{P} \parallel \mathbb{P}')}{\log 2}, \quad d \in [0, 1].$$

As drift is measured based on the differences between distributions, a critical challenge is effectively mapping data or workloads to their corresponding distributions, denoted as \mathbb{P} . For data, we consider a relational database \mathbf{R} containing multiple tables, each comprising a set of attributes. To approximate the distribution $\mathbb{P}_{\mathbf{R}}$, we decompose the joint distribution into their marginal attribute distributions, *i.e.*, $\mathbb{P}_{\mathbf{R}}(A_1, A_2, \dots, A_m) \approx \prod_{i=1}^m \mathbb{P}(A_i)$, where $\mathbb{P}(A_i)$ represents the distribution of the i -th attribute. We would like to note that measuring the distance between marginal distributions remains an effective approach to quantifying overall distributional drift, regardless of underlying correlations, as our focus is solely on capturing distributional differences. We exclude primary keys and attributes with unique constraints from the distribution computation, as their values are inherently uniform or deterministic. For the remaining attributes, we employ specific strategies based on their data types to approximate their distributions. Categorical attributes (*e.g.*, CHAR, VARCHAR) and discrete numerical values are handled by computing distributions over all observed values in the table. For example, if a column contains values A, B, C , we calculate the probability of each value occurring: $\Pr(A), \Pr(B), \Pr(C)$. Continuous numerical attributes are approximated by discretizing values into a fixed number of bins. The corresponding distribution is then estimated by computing the probability density of each bin. This binning strategy is commonly employed in database histograms to estimate attribute distributions and query selectivity. Moreover, the number and range of bins are determined based on the observed value range to balance precision and computational efficiency. For example, a numerical column with values in the range $[0, 100]$ can be divided into 10 bins, and the frequency of values in each bin determines the distribution.

For a workload consisting of N queries $\mathbf{Q} = \{\mathbf{q}_1, \mathbf{q}_2, \dots, \mathbf{q}_N\}$, we define the workload distribution $\mathbb{P}_{\mathbf{Q}}$ as the distribution over *query templates*. Specific features, such as query patterns, query arrival rates, *etc.*, characterize each query template. To model query patterns and arrival rates in a unified manner, we define a workload table with 3 attributes: Join Pattern, Predicate, and Query Interval. The Join Pattern and Predicate columns capture the query pattern, representing table join patterns (*e.g.*, $r_1 \bowtie r_2$), and predicates (*e.g.*, Bal = '10K'). The Query Interval column quantifies the arrival rate by recording the time gap between consecutive queries. We control the distributions of the workload table to synthesize workloads with query pattern drift, arrival rate drift, or both, while preserving the

inherent correlations. For example, we can introduce a workload, where queries with a certain join pattern become more frequent, while simultaneously increasing the corresponding query arrival rates by reducing the query interval (*e.g.*, from 2.0s to 0.5s), thereby inducing drift in both query patterns and arrival rates. Note that the workload table used here is for illustration purposes; it can be extended with additional attributes for more complex queries.

4.2 Drift-aware Data and Workload Generation

After defining the drift factor d , the next problem is to generate drifted data and workloads that satisfy a specified d . To address this, we first provide a formal problem definition and then explain how to construct the drift-aware data and workload generator.

4.2.1 Problem Definition. We define a database running in a time window \mathbf{T} with $N(N \geq 2)$ time slots, *i.e.*, $\mathbf{T} = (ts_1, ts_2, \dots, ts_N)^\top$. Recall that we denote \mathbf{R} and \mathbf{Q} as random variables of the data and workload in the database, respectively, and we map them to their underlying distributions $\mathbb{P}_{\mathbf{R}}^{(i)}$ and $\mathbb{P}_{\mathbf{Q}}^{(i)}$ at ts_i . Formally, we define the drift-aware data and workload generation below.

Definition 4 (Drift-aware Data and Workload Generation). Given a series of drift factors $\mathbf{D} = (d_1, d_2, \dots, d_N)^\top$, where each drift factor d_i quantifies the degree of change in the distribution between adjacent time slots (ts_j, ts_i) . The distribution of either data or workload at time ts_j is obtained by transforming the distribution at time ts_i with a function g , according to the drift factor d_i :

$$\mathbb{P}_{\mathbf{R}}^{(j)} = g_{\mathbf{R}}(\mathbb{P}_{\mathbf{R}}^{(i)}, d_i, C), \quad \mathbb{P}_{\mathbf{Q}}^{(j)} = g_{\mathbf{Q}}(\mathbb{P}_{\mathbf{Q}}^{(i)}, d_i, C),$$

where C is the corresponding inherent correlations, and $g_{\mathbf{Z}} : \Omega_{\mathbf{Z}} \times [0, 1] \times C \rightarrow \Omega_{\mathbf{Z}}$ is the drift function applied on input space \mathbf{Z} , transforming its distribution on the same domain.

Given a distribution $\mathbb{P}^{(i)}$ and the drift factor d_i , the generated new distribution $\mathbb{P}^{(j)}$ should 1) exhibit drift quantified by d from $\mathbb{P}^{(i)}$; and 2) preserve inherent correlations C . Mathematically, this is equivalent to finding a hypersurface in $\Omega_{\mathbf{Z}}$, the domain of input space \mathbf{Z} (*i.e.*, either data and workload), which satisfies the equation:

$$d(\mathbb{P}_i, \mathbb{P}_j) \approx d^* \quad \text{subject to} \quad C(\mathbb{P}_j) \approx C(\mathbb{P}_i). \quad (1)$$

However, there are infinite solutions to Equation 1, which makes it difficult to interpret and control. To solve this, we limit the expressiveness of \mathbb{P}_j through a DDPM-based generator.

4.2.2 Drift-aware Data and Workload Generator Construction. We now introduce the design of our proposed drift-aware data and workload generator, which synthesizes drifted data and workloads while preserving inherent correlations. Below, we present the theoretical foundations, describe the generator's training mechanism, and illustrate the complete generation process.

Theoretical Analysis. Given a desired drift factor d , our objective as outlined in Section 4.2.1 to generate the drifted data \mathbf{x}_{drift} can be expressed as sampling from $p(\mathbf{x}_{t-1} | \mathbf{x}_t, d)$, a conditional DDPM reverse distribution that incorporates the desired drift d . As outlined in Section 2.3, $p(\mathbf{x}_{t-1} | \mathbf{x}_t, d)$ can be decomposed as:

$$p(\mathbf{x}_{t-1} | \mathbf{x}_t, d) \propto p(\mathbf{x}_{t-1} | \mathbf{x}_t) \Pr(d | \mathbf{x}_{t-1}, \mathbf{x}_t), \quad (2)$$

where $p(\mathbf{x}_{t-1} | \mathbf{x}_t)$ can be modeled by the denoising process of DDPM, *i.e.*, $p(\mathbf{x}_{t-1} | \mathbf{x}_t) = \mathcal{N}(\mathbf{x}_{t-1}; \boldsymbol{\mu}(\mathbf{x}_t, t; \theta), \sigma_t^2 \mathbf{I})$, and $\Pr(d | \mathbf{x}_{t-1}, \mathbf{x}_t)$

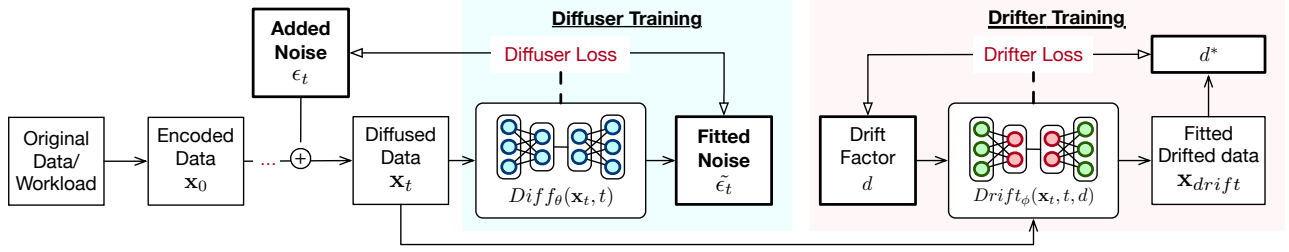


Figure 2: Diffuser and Drifter Training

guides the process to introduce the specified drift d . Since the drifted data \mathbf{x}_{drift} is the target output, Equation (2) can be rewritten as:

$$p(\mathbf{x}_{t-1}|\mathbf{x}_t, \mathbf{x}_{drift}) \propto p(\mathbf{x}_{t-1}|\mathbf{x}_t)\Pr(\mathbf{x}_{drift}|\mathbf{x}_{t-1}, \mathbf{x}_t). \quad (3)$$

Note that the mean of the Gaussian distribution, $\boldsymbol{\mu}(\mathbf{x}_t, t; \theta)$, determines the trajectory of the denoising process [11, 36]. We therefore leverage $\Pr(\mathbf{x}_{drift}|\mathbf{x}_{t-1}, \mathbf{x}_t)$ to introduce a controlled drift to the mean $\boldsymbol{\mu}$.

Theorem 1. The controlled reverse distribution $p(\mathbf{x}_{t-1}|\mathbf{x}_t, \mathbf{x}_{drift})$ is able to be approximated using $\Pr(\mathbf{x}_{drift}|\mathbf{x}_t)$ and its gradient at \mathbf{x}_t , or $\nabla_{\mathbf{x}_t}\Pr(\mathbf{x}_{drift}|\mathbf{x}_t)$.

PROOF. For Equation (3), the first part is approximated by a Gaussian model, while the second part can be simplified using conditional independence, which transforms the equation to:

$$p(\mathbf{x}_{t-1}|\mathbf{x}_t, \mathbf{x}_{drift}) \approx z\mathcal{N}(\mathbf{x}_t; \boldsymbol{\mu}, \Sigma)\Pr(\mathbf{x}_{drift}|\mathbf{x}_t),$$

where z is the normalizing factor. Next, as proven by Dickstein et al. [47], we can perform Taylor expansion around $\boldsymbol{\mu}$ to further approximate $p(\mathbf{x}_{t-1}|\mathbf{x}_t, \mathbf{x}_{drift})$ so that a perturbed Gaussian distribution can be used to model it:

$$\begin{aligned} \log p(\mathbf{x}_{t-1}|\mathbf{x}_t, \mathbf{x}_{drift}) &\approx \log \mathcal{N}(\mathbf{x}_t; \boldsymbol{\mu}, \Sigma) + \log \Pr(\mathbf{x}_{drift}|\mathbf{x}_t) \\ &\approx -\frac{1}{2}(\mathbf{x}_t - \boldsymbol{\mu})^\top \Sigma^{-1}(\mathbf{x}_t - \boldsymbol{\mu}) + (\mathbf{x}_t - \boldsymbol{\mu}) \cdot \mathbf{g} + C \\ &= -\frac{1}{2}(\mathbf{x}_t - \boldsymbol{\mu} - \Sigma \cdot \mathbf{g})^\top \Sigma^{-1}(\mathbf{x}_t - \boldsymbol{\mu} - \Sigma \cdot \mathbf{g}) + C \\ &= \log \mathcal{N}(\mathbf{x}_t; \boldsymbol{\mu} + \Sigma \cdot \mathbf{g}, \Sigma), \end{aligned}$$

where $\mathbf{g} = \nabla_{\mathbf{x}_t}\Pr(\mathbf{x}_{drift}|\mathbf{x}_t)$, and the constant term C can be ignored. In other words, $p(\mathbf{x}_{t-1}|\mathbf{x}_t, \mathbf{x}_{drift})$ can be approximated by $\mathcal{N}(\mathbf{x}_t; \boldsymbol{\mu} + \Sigma \cdot \nabla_{\mathbf{x}_t}\Pr(\mathbf{x}_{drift}|\mathbf{x}_t), \Sigma)$. \square

Conceptually, Theorem 1 ensures the generated data moves toward the target drifted distribution. We therefore design a generation framework comprising two key components: the diffuser and the drifter. The diffuser learns the distribution of original data and workloads, while the drifter guides the generation process to introduce specified drift.

Diffuser and Drifter Training. We illustrate the training process of the diffuser and drifter in Figure 2. The diffuser serves as the core generative model, learning to approximate the unconditional distribution $p(\mathbf{x}_{t-1}|\mathbf{x}_t)$. To achieve this, we train the diffuser to predict the mean $\boldsymbol{\mu}(\mathbf{x}_t, t; \theta)$ of the reverse denoising process, which is directly related to the noise added during the forward process. In particular, the reverse process can be rewritten in terms of noise ϵ_t , where: $\boldsymbol{\mu}(\mathbf{x}_t, t; \theta) = \frac{1}{\sqrt{\alpha_t}}(\mathbf{x}_t - \sqrt{1 - \alpha_t} \cdot \epsilon_t)$, and α_t is a parameter

derived from the variance schedule σ_t . This formulation makes noise reconstruction a central task in training, and thus, the diffuser is trained by minimizing the noise reconstruction error:

$$\mathcal{L}_{Diff} = \mathbb{E}_t [\|\epsilon_t - Diff(\mathbf{x}_t, t)\|^2],$$

where $Diff(\mathbf{x}_t, t)$ is the noise prediction output of the diffuser at timestep t .

The drifter, represented as $Drift(\mathbf{x}_t, t, d)$, is then utilized to fit $\Pr(\mathbf{x}_{drift}|\mathbf{x}_t)$ to generate \mathbf{x}_{drift} with the same size as the current noisy data \mathbf{x}_t , and satisfies the user-specified drift factor d . It is trained using a composite loss function that balances the drift-introduction accuracy and the preservation of original correlations:

$$\mathcal{L}_{Drift} = \mathbb{E}_{t, d^*} [\|d(\mathbf{x}_{drift}, \mathbf{x}_t) - d^*\|_2^2 + \lambda \|C(\mathbf{x}_{drift}) - C(\mathbf{x}_t)\|_2^2],$$

where the first Mean Square Error (MSE) part ensures that the JS divergence of the distributions between the drifted and the current-step result closely matches any drift factor d^* , and the second MSE part penalizes any deviation in the correlations of the two distributions. The hyperparameter λ balances their importance.

Generation Process. Synthesizing drifted data and workloads involves iterative timesteps involving the diffuser and the drifter, as shown in Figure 1. After sampling an initial noise $\mathbf{x}^T \sim \mathcal{N}(0, \mathbf{I})$, the diffuser transforms \mathbf{x}^T into drifted data $\tilde{\mathbf{x}}_0$ over T discrete timesteps. At each step t , the drifter computes a gradient $\mathbf{g}_t = \nabla_{\mathbf{x}_t}\Pr(\mathbf{x}_{drift}|\mathbf{x}_t) = \nabla_{\mathbf{x}_t}Drift(\mathbf{x}_t, t, d)$, which adjusts the predicted mean $\tilde{\boldsymbol{\mu}}_t = \boldsymbol{\mu} + \Sigma \cdot \mathbf{g}_t$, and use the adjusted mean $\tilde{\boldsymbol{\mu}}_t$ to sample the next state \mathbf{x}_{t-1} . We repeat this process for timesteps $t = T, T-1, \dots, 1$, gradually refining \mathbf{x}_t toward \mathbf{x}_{drift} . After decoding \mathbf{x}_{drift} , we obtain the drifted data or workload that reflects the desired drift while maintaining the inherent correlations.

4.2.3 Preserving Temporal Constraints. Real-world data rarely makes abrupt, arbitrary transitions; rather, it evolves in a manner consistent with observed temporal constraints. To ensure our generator respects these constraints, we propose an *agent-based* selection mechanism that chooses an appropriate generator from a pool of snapshot-specific models. In this way, any generated drifted data and workload follow plausible historical progressions rather than leaping to distributions that never occurred in practice. Specifically, we first partition the historical timeline into snapshots, each capturing data from a certain period or system phase (e.g., Snapshot 1 for early behavior, Snapshot 2 for mid-range drift, and so on). For each snapshot S_i , we train a distinct generative model \mathcal{G}_i that learns the empirical distribution in that time segment. These snapshot-specific models collectively form a library $\{\mathcal{G}_1, \mathcal{G}_2, \dots\}$,

where each \mathcal{G}_i is specialized to generate data or workload consistent with the distribution observed in its corresponding time window. We then introduce an *agent* to choose which model in the library to invoke when asked to produce drifted data. Concretely, upon receiving a request specifying: 1) an original dataset (or baseline distribution \mathbb{P}), 2) a desired drift factor d that quantifies how far the new data should deviate from \mathbb{P} , the agent measures how close d is to each snapshot’s drift range. For instance, we can compute a distance metric $\text{dist}(d, \alpha_i)$ between the requested drift d and the average (or representative) drift α_i of each snapshot S_i . The agent then selects the generator \mathcal{G}_{i^*} with the minimal distance: $\mathcal{G}_{i^*} = \arg \min_{\mathcal{G}_i} \text{dist}(d, \alpha_i)$. By choosing \mathcal{G}_{i^*} , the system ensures that newly generated data aligns with a distribution known to have occurred naturally in the historical timeline, rather than fabricating an unobserved or infeasible distribution. This snapshot-driven mechanism implicitly preserves *temporal constraint* because any requested drift level d is mapped to one of the valid distributions. If a drift beyond all observed snapshots is requested (i.e., no model in $\{\mathcal{G}_i\}$ matches well), the agent can either: 1) *reject* the request as falling outside real-world evolution patterns, or 2) apply an *extrapolation* step, such as linear interpolation among multiple snapshot models, ensuring the resulting distribution is still anchored to plausible historical transitions. Because unseen or extreme values cannot be arbitrarily generated, the possibility to produce data violating natural progression is greatly reduced. In effect, the agent-based selection corroborates that a dataset with drift d is one that could appear either after or before \mathbb{P} in a genuine temporal sequence.

5 BENCHMARKING PREPARATION

In this section, we first revisit the general frameworks and key design choices of three representative learned database component categories, namely end-to-end learned query optimizers, updatable learned indexes, and learned concurrency control. Then, we describe the implementation of NeurBench.

5.1 Learned Database Components Revisited

5.1.1 End-to-end Learned Query Optimizer. The general framework of end-to-end learned query optimizers is shown in Figure 3. Given a query q , the optimizer first performs *plan search* to obtain a set of candidate query plans $P(q) = \{p_0, p_1, \dots, p_N\}$, and then conducts *plan selection* to choose one or top- k plans from $P(q)$ for real execution. During the plan search and selection, it interacts with an *ML model* to assess the plan quality. Using the real execution statistics of chosen plans as training data, the model is periodically retrained or fine-tuned to adapt to data and workload drift. Consequently, the performance of a learned query optimizer is determined by the design of its plan search, plan selection, and ML model.

Model. There are two main types of models for assessing plan quality: 1) *Regression model* predicts the execution cost or latency $\hat{L}(p)$ of a given plan p , optionally providing a confidence score $C(p)$ that reflects the model’s certainty, i.e., $f_{qo}(p) = (\hat{L}(p), C(p))$ [39, 40, 63]. 2) *Ranking model* predicts a binary ranking value r for two given plans p_1 and p_2 , where $r = 1$ if p_1 is expected to outperform p_2 , and $r = 0$ otherwise, i.e., $f_{qo}(p_1, p_2) = r, r \in \{0, 1\}$ [66]. We note that since a query plan can be represented as a tree, these models are typically implemented with one of two structures: Tree-CNN [42] and

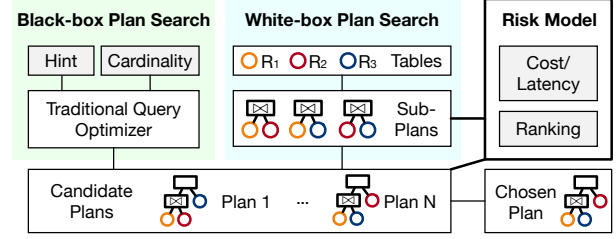


Figure 3: End-to-end Learned Query Optimizers

Tree-LSTM [49]. Both structures are deep neural networks designed for tree structures to capture bottom-up sequential information.

Plan Search. There are two paradigms in plan search, which differ in whether they rely on traditional query optimizers: 1) *Black-box search* provides auxiliary information to traditional query optimizers for candidate plan generation. Based on the type of information provided, it can be further categorized into: (a) *Hint-based*. It supplies hints (parameters that control physical operators, such as join or scan types) to the traditional optimizer, guiding it to generate corresponding query plans [39, 63]. Selecting proper hints is therefore important for the quality of the candidate plan set. Early approaches [39] determine static hint sets in advance by database experts with in-depth knowledge of query optimization. Some recent methods are proposed to dynamically select hints based on search algorithms [1, 63]. For example, HybridQO [63] uses a Monte Carlo tree search combined with a join order prediction model to generate a set of potential join orders as hints. AutoSteer [1] automatically discovers hints that can impact a given query through a greedy search of the hints supported by the database. (b) *Cardinality-based*. It adjusts (by magnifying or reducing) estimated cardinalities multiple times to generate a variety of candidate plans [66]. 2) *White-box search* embeds the model directly into the plan search process without relying on the traditional optimizers [40]. It starts with an empty or partial plan and iteratively constructs a complete query plan until a predefined number of candidate plans is reached. At each step, multiple subplans are generated. After using an ML model to evaluate their quality, ineffective subplans are pruned while the remaining ones are expanded in subsequent iterations.

Plan Selection. Based on the cost/latency or ranking predicted by the model, the optimizer selects plans for execution from the candidate set, following one of these strategies: 1) *Best-only*, which only selects the plan with the lowest predicted cost/latency or highest ranking. 2) *Top-k*, which selects the best plan along with the next $k-1$ highest-ranked plans. These $k-1$ plans are executed asynchronously in the background to gather more real execution data. Adjusting k controls the balance between exploiting the best-known plan and exploring alternative plans.

5.1.2 Updatable Learned Index. Given a search key k , the learned index f_{idx} predicts its position $\hat{PS}(k)$ in the data table, i.e., $f_{idx}(k) = \hat{PS}(k)$. Learned indexes typically organize a set of ML models in a layered structure, where each node contains a model for position prediction. To handle key insertions, the structure must be updatable where nodes can be added or deleted dynamically. Therefore,

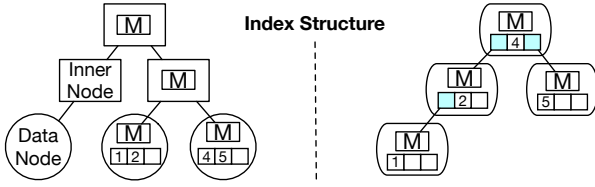


Figure 4: Structures of Existing Learned Indexes

the design of the index structure and update mechanism are key factors influencing the performance of learned indexes.

Index Structure. As shown in Figure 4, existing learned indexes can be classified into two representative structures, based on whether they have different node types: 1) *Heterogeneous structure*. It consists of two distinct types of nodes: inner nodes and leaf nodes. Inner nodes do not store data, whereas leaf nodes store the actual data. Given a query key, inner nodes predict the next step in the structure, directing the query to the appropriate leaf node, where a search is performed to locate the exact position of the key. 2) *Homogeneous structure*. Every node in this structure is responsible for storing part of the data. Given a query key, each node predicts whether the key falls within its stored data, or if the query should proceed to a corresponding child node.

Structural Update. The key insertion can trigger index structural updates. There are two main update mechanisms, which differ in how they handle incoming keys: 1) *In-place*. Index nodes reserve gaps (empty slots), which allow new keys to be directly inserted into the index structure. Given a new key, the index first locates an appropriate position for insertion. However, conflicts can occur when multiple keys are mapped to the same position, as the model was trained without the new key, or if the predicted slot is already occupied. In such cases, conflict resolution is required, typically following one of these two methods: (a) *Shift method*, sequentially moving the existing key to the nearest available gap to create space at the target location for successful insertion [13]; (b) *Chain method*, creating a new node for the conflicting target position and inserting the key into this new node [60]. 2) *Delta-buffer*. One or more dedicated buffers are created separately from the index structure. When a new key arrives, it is first placed in the buffer and periodically merged into the index structure. The buffer can be organized at two different levels of granularity: (a) *Tree-level buffer*. A single buffer is maintained for the entire index [14]; (b) *Node-level buffer*. Each node has its own dedicated buffer [50].

5.1.3 Learned Concurrency Control (CC). Learned CC algorithm dynamically selects the most suitable CC actions based on the current workload to optimize transaction performance. It takes a transaction operation op (e.g., read or write) and the current system condition $C(op)$ (e.g., contention levels) as inputs, and leverages an ML model f_{cc} to predict the most appropriate CC action for the operation op . These actions may include acquiring a shared lock, acquiring an exclusive lock, processing without locking, etc. Formally, let \mathbf{A} be the set of available CC actions, f_{cc} can be defined as $f_{cc}(op, C(op)) = a$, where $a \in \mathbf{A}$. As new operation types emerge or system conditions change, the learned CC algorithm requires re-training to adapt to workload drift. PolyJuice [53], a state-of-the-art learned CC algorithm is proposed following this definition, which

Table 1: A Taxonomy of Evaluated Learned Components

	Method	Model	Plan Search	Plan Selection
End-to-end	HybirdQO [63]	Regression	Hint-based	Top-k
Learned Query	Bao [39]	Regression	Hint-based	Best-only
Optimizer	Neo [40]	Regression	Write-box	Best-only
	Lero [66]	Ranking	Cardinality-based	Top-k
	Method	Structure	Structural Update	
Updatable	ALEX [13]	Heterogeneous	In-place (Shift)	
Learned Index	LIPP [60]	Homogeneous	In-place (Chain)	
	XIndex [50]	Heterogeneous	Delta-buffer (Node-level)	
	PGM-Index [14]	Heterogeneous	Delta-buffer (Tree-level)	
Learned CC	PolyJuice [53]			

predicts CC actions for each unique operation within a transaction. Furthermore, to adapt to workload drift, PolyJuice performs full retraining based on historical workload traces and applies the updated model to handle future workloads.

5.2 Implementation of NeurBench

We build upon the diffusion model code from existing works [22, 36] to implement the drift-aware data and workload generator of NeurBench. In particular, we implement the diffuser based on a Multilayer Perceptron (MLP) with hidden layer dimensions of (512, 1024, 1024, 512) and the drifter as a similar MLP with hidden layer dimensions of (512, 512). We use table formats to represent both data and workloads, as specified in Section 4.1, and encode the table using the analog bit encoding technique [36]. For each table, we dynamically adjust the learning rate from $1e^{-4}$ to $2e^{-3}$ to ensure the convergence of the training process.

NeurBench imposes no constraints on the choice of its evaluators and is flexible in supporting various implementations. Since no existing database system seamlessly integrates all tested learned database components, we use separate evaluators for each type of learned component. We adopt existing learned database component evaluators [27, 48, 53] and extend them to support evaluation under data and workload drift scenarios. The source code of NeurBench is available at [43].

6 EVALUATION

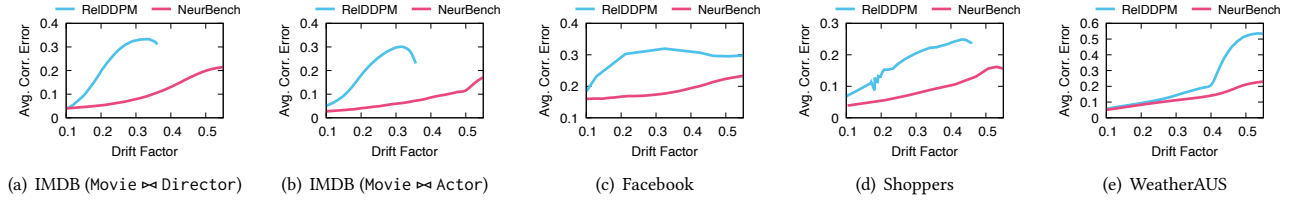
In this section we evaluate the effectiveness of NeurBench in generating drifted data and workloads, and then benchmark selected learned query optimizers, learned indexes and learned CC.

6.1 Experimental Setup

6.1.1 Competitors. We compare the data generator of NeurBench with ReIDDPM, a state-of-the-art data synthesis framework, and use NeurBench to evaluate representative learned database components as summarized in Table 1.

ReIDDPM [36] is a state-of-the-art DDPM-based data synthesis framework. We chose ReIDDPM as a competitor because it also uses guided diffusion and achieves effective correlation-preserved data generation. Since ReIDDPM does not natively support drift-aware data generation, we extend ReIDDPM by adjusting the strength of the guidance in the denoising process to generate drifted data.

Representative Learned Database Components. Based on the analysis in Section 5.1, we carefully select learned database components that cover most key design choices for our evaluation, as


Figure 5: Performance on Generating Drifted Datasets with Varying Drift Factors

listed in Table 1. Due to space constraints, we opt not to conduct exhaustive evaluations of all existing learned database components.

6.1.2 Datasets and Workloads. We construct an original dataset and workload, and use NeurBench to generate corresponding drifted datasets and workloads for our experiments.

Original Dataset and Workload. We use the Internet Movie Database (IMDB) [20], a real-world dataset containing 21 tables with intricate inter-table and intra-table correlations. Based on IMDB, we construct a combined workload to conduct our experiments. As different learned database components may vary in their requirements of workloads, we accommodate three types of operations in the workload, as listed below: 1) *Complex queries*. We include all 113 queries from JOB [28], a widely-used workload for query optimizer evaluation [5, 27]. It is derived from 33 real query templates, covering complex query patterns that access 4 to 17 IMDB tables. 2) *Range scans*. Each scan operation queries a range [start_key, end_key] on the ID attribute of the IMDB Name table, which contains 4M records. By default, start_key is randomly selected from the entire table, and the scan length (i.e., end_key - start_key) is randomly selected between 1 and 100, following prior studies [48, 60]. 3) *Transactions*. We execute concurrent transactions on the IMDB Name table. By default, each transaction consists of 5 reads and 5 writes, following previous works [8, 17, 53]. Each read or write is performed on a randomly selected record.

Drifted Datasets and Workloads. To evaluate learned database components under various drift scenarios, we employ NeurBench to generate drift datasets and workloads from the original dataset and workload based on a given drift factor d . We collect historical IMDB datasets from [2] and feed them into the generator to preserve temporal constraints. We denote no drift as $d=0$, indicating that the original dataset and workload are used. We apply drift factors of 0.1, 0.3, and 0.5 ($d \in \{0.1, 0.3, 0.5\}$) to simulate mild, medium, and severe drift. In particular, we use the following drifted data and workloads: 1) *Drifted IMDB*, the dataset drifts from the original IMDB with d . 2) *Workload with join pattern drift*, the workload with drift in query join patterns according to d ; 3) *Workloads with predicate drift*, the workload with drift in query predicates; 4) *Workloads with arrival rate drift*, the workload with transaction arrival rate drift.

We also employ an extended version of CH-Benchmark, which includes drifted workloads generated by NeurBench, to conduct our experiments.

CH-Benchmark [7]. CH-Benchmark is a hybrid benchmark combining TPC-C [9], a standard transactional benchmark, and TPC-H [10], a standard analytical benchmark. CH-Benchmark integrates the tables from both benchmarks and consists of all TPC-C transactions and all TPC-H queries. Its transactional workload comprises 5 types of transactions, with NewOrder and Payment accounting

for 45% and 43% respectively, and each of the other three transaction types contributing 4%. In addition, its analytical workload includes 22 analytical queries characterized by complex query patterns. We use NeurBench to generate transactional workloads with arrival rate drift, as well as analytical workloads with mixed drift (including both join portion drift and predicate drift).

6.1.3 Evaluation Metrics. We assess the effectiveness of data synthesis using *average correlation error*, which measures the average deviation in correlations between the generated dataset and the original dataset across all attributes. Correlations are computed using Pearson’s correlation coefficient [57].

For learned database components, we assess their performance using *execution time* and *throughput*, where execution time (*EXE*) refers to the time taken for a query, and throughput (*TPS*) measures the number of queries/transactions processed per second. To quantify performance degradation under drift, we introduce two additional metrics: 1) *Performance Regression*, which measures the relative increase in execution time as $(EXE_d - EXE_{d=0})/EXE_{d=0}$, and 2) *Throughput Drop*, which captures the percentage decrease in throughput as $(1 - TPS_d/TPS_{d=0}) \times 100\%$. Both performance regression and throughput drop indicate higher performance degradation with larger values, and therefore, we use them to directly reflect the impact of drift across different learned database components.

6.1.4 Default Configuration. We conduct experiments on 2 servers equipped with an Intel(R) Xeon(R) W-1290P CPU@ 3.70GHz (10 cores, 20 threads), 128 GB memory, and 3 NVIDIA GeForce RTX 2080 Ti GPUs. All experiments are run within Docker containers (Ubuntu 22.04 with CUDA 11.8.0). We deploy NeurBench on one machine as the client and the learned database components on another machine to prevent local resource contention. Unless otherwise specified, we use the default parameters stated in the adopted evaluators [27, 48, 53] for our experiments.

6.2 Evaluation on Drift-aware Data and Workload Generation Framework

In this set of experiments, we evaluate the effectiveness of our proposed drift-aware data and workload generation framework by comparing NeurBench with RelDDPM.

6.2.1 Experiments on generating drifted datasets, under varying drift factors. We first assess the correlation error of drifted IMDB datasets with the drift factor increasing from 0.1 to 0.5. Following RelDDPM, we join multiple IMDB tables and measure both inter-table and intra-table correlations on the joined tables. Specifically, we construct two joined tables: 1) *Movie ⇨ Director*, where movies are linked to directors via director ID; and 2) *Movie ⇨ Actor*, where

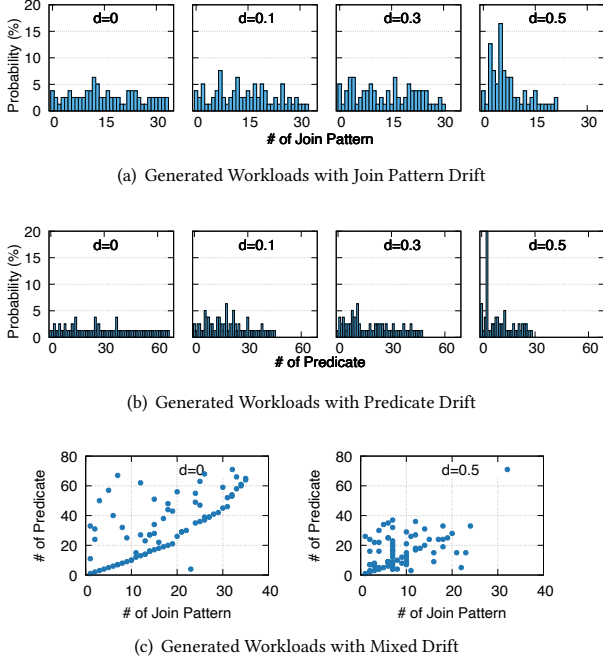


Figure 6: Performance on Generating Drifted Workloads with Varying Drift Factors

movies are linked to actors via actor ID. We plot the average correlation error of these two joint tables in Figure 5(a) and Figure 5(b), respectively. We can observe that NeurBench consistently achieves lower average correlation errors than RelDDPM across all drift factors, with the correlation error increasing nearly linearly as the drift factor grows. In contrast, RelDDPM fails to generate data for drift factors greater than 0.4, and its correlation error fluctuates unpredictably, showing no clear relationship with the drift factor. These results demonstrate that due to our proposed drift-aware data generation framework, NeurBench can effectively synthesize drifted data while preserving correlations in a controlled manner.

We then study the general applicability of NeurBench in synthesizing drifted data. To this end, we utilize NeurBench to generate drifted data for three additional real-world datasets, including Facebook [16], Shopper [46], and WeatherAUS [56]. As shown in Figure 5(c), Figure 5(d), and Figure 5(e), NeurBench consistently achieves lower average correlation error than RelDDPM across different datasets and drift factors. Moreover, NeurBench maintains a controlled increase in correlation error as the drift factor increases, whereas RelDDPM exhibits erratic correlation errors and struggles to generate drifted data for high drift factors. We therefore confirm the ability of NeurBench to generate data with controlled drift while preserving correlation, demonstrating its effectiveness in generating drifted data across different datasets.

6.2.2 Experiments on generating drifted workloads, under varying drift factors. We now evaluate NeurBench in generating drifted workloads, with drift factors $d=0.1$, $d=0.3$, and $d=0.5$. We first assess the effectiveness of generating drifted workloads with join pattern drift by measuring the probability distribution of each join pattern,

where probability refers to its proportion in the generated workload. In this section, we use the complex queries indicated in Section 6.1.2 as the original workload. The results in Figure 6(a) indicate that, as the drift factor increases, the distribution becomes more skewed compared to the original workload ($d=0$). In addition, under larger drift ($d=0.5$), some join patterns in the original workload may disappear in the drifted workload. Therefore, we demonstrate that NeurBench can effectively generate a drifted workload that can be used to simulate a realistic drift scenario where learned components may encounter unseen query patterns. We then evaluate the performance of generating workloads with predicate drift. Figure 6(b) shows that predicate pattern distributions follow a consistent trend, *i.e.*, higher drift factors result in more skewed distributions. These results validate the effectiveness of NeurBench in synthesizing drifted workloads across different types.

We also evaluate NeurBench’s ability to generate workloads with mixed drift. Specifically, we generate workloads exhibiting both join pattern drift and predicate drift with certain correlation, and visualize the distribution of queries across different join patterns and predicates in Figure 6(c). The results show that the query distribution becomes more skewed as the drift factor increases, with fewer distinct categories appearing.

6.3 Evaluation on Learned Query Optimizers

Here we evaluate selected learned query optimizers, *i.e.*, Bao [39], HybridQO [63], Lero [66], and Neo [40], under various data and workload drift scenarios. We use the complex queries in the workload specified in Section 6.1.2 to perform this set of experiments. In particular, we construct a testing set of 33 queries from the original 113 queries by ensuring all 33 query templates are included. Since all these learned optimizers are integrated with PostgreSQL, we also include PostgreSQL using its traditional optimizer as a reference baseline. The datasets, workloads, and the corresponding training and evaluation processes are specified in the following sections.

6.3.1 Experiments on the complex queries, under data drift with varying drift factors. Given a drift factor d , we first train each learned optimizer with the drifted IMDB datasets corresponding to d and the original workload, and then execute all the queries in the testing set on the original dataset. We plot the total execution time of these queries in Figure 7(a), and use Figure 7(b) to show the corresponding performance regression (defined in Section 6.1.3) under varying drift factors. We report our observations below:

O1: None of the evaluated learned optimizers outperform PostgreSQL under data drift. This is due to the fact that most learned optimizers depend on the ML model for accurate query plan quality assessment. When data distributions drift, the models can become less reliable, leading to suboptimal plan selection.

O2: HybridQO, Neo, and Bao exhibit performance regression with increased data drift, while the performance regression of Lero is negligible. This can be attributed to the fact that HybridQO, Neo, and Bao rely on ML models that learn query plan execution times from historical executions. Since execution time is susceptible to data distribution drift, their learned models can struggle to generalize under drift. In contrast, Lero, which adopts a ranking-based model, demonstrates better robustness to data

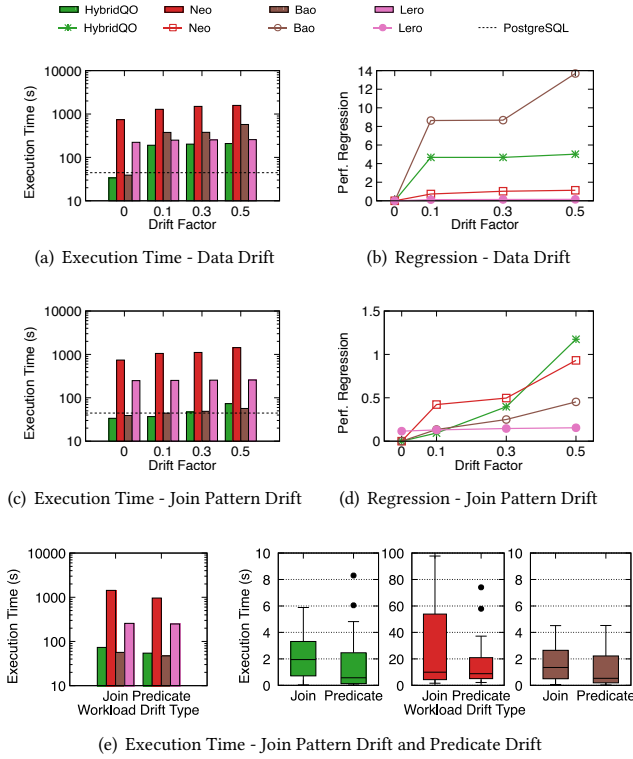


Figure 7: Performance of Learned Query Optimizers under Data Drift, Join Pattern Drift, and Predicate Drift with Varying Drift Factors

drift, as the relative ranking can be more stable than exact execution time predictions. Further, the stable performance of Lero also stems from its cardinality-based plan search. While cardinality for a certain query may change with drift, Lero may have already encountered similar plans with changed cardinality during training, thus enhancing its adaptability to data drift.

O3: Bao experiences the highest performance regression under data drift, followed by HybridQO and then Neo. Bao relies entirely on best-only plan selection, whereas HybridQO explores a top-k plan strategy. As a result, HybridQO may have learned suboptimal plans for certain data distributions that become more effective under drifted data, making it more generalizable than Bao. Unlike Bao and HybridQO, Neo learns the cost of each subquery, which tends to be more stable under data drift since subquery cost estimation is less affected by global data distribution drift.

6.3.2 Experiments on the complex queries, under workloads with various join pattern drift and predicate drift. We train each learned optimizer with the original data and the workloads with join pattern drift corresponding to drift factor d , and then execute the queries in the testing sets. We report the total execution time of these queries in Figure 7(c) and the corresponding performance regression under varying drift factors in Figure 7(d). We can observe that:

O4: Join pattern drift affects the performance of HybridQO, Neo, and Bao more significantly than Lero. HybridQO and Bao become ineffective under higher join pattern drift because they both rely on hints to generate query candidates, preventing them

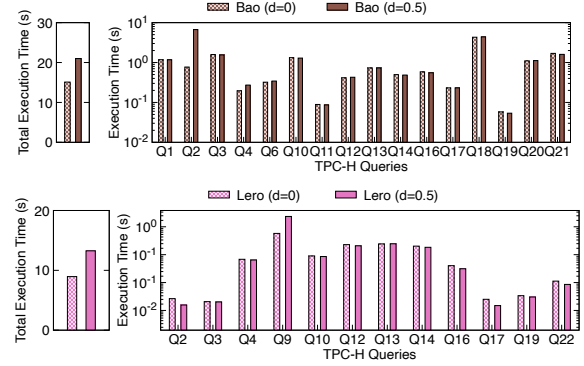


Figure 8: Performance Evaluation of Learned Query Optimizers using Drifted CH-Benchmark Workload

from adapting to unseen join patterns and leading to inaccurate latency predictions. Neo, which employs a white-box plan search with a best-only plan selection strategy, is more susceptible to local optima and thus struggles to explore globally optimal plans under join pattern drift. In contrast, as discussed in O2, Lero generates candidate plans by varying cardinality estimations, enabling it to better tolerate join pattern drift.

We then fix the drift factor d to 0.5 and conduct experiments on workloads with join pattern drift and predicate drift to investigate the performance of learned query optimizers under different types of workload drift. Each learned optimizer is trained on the original data with the drifted workload and then evaluated using the same set of testing queries. The results in Figure 7(e) show that:

O5: HybridQO and Neo are more sensitive to join pattern drift than Bao. HybridQO relies on join-order-based hints, making it more susceptible to changes in join patterns, whereas Bao uses more general hints that incorporate both join patterns and predicates, allowing it to adapt better to such drift. Further, as discussed in O3, Neo learns the cost of subqueries individually. While this makes it more stable under data drift, it increases its sensitivity to query pattern drift, including changes in join patterns.

6.3.3 Experiments on CH-Benchmark workload with mixed drift. We now evaluate Bao and Lero using the CH-Benchmark workload specified in Section 6.1.2. We exclude other learned query optimizers because their implementations have specific requirements on the query format, and modifying their code to handle analytical queries in CH-Benchmark is cumbersome. For the evaluation, we generate workloads exhibiting mixed drift (combining both join-pattern drift and predicate drift) with drift degree $d = 0.5$. We then measure and compare the execution times for the original queries ($d = 0$) and the drifted queries ($d = 0.5$). Queries unsupported by Bao and Lero are omitted from the analysis. The results, plotted in Figure 8, indicate that workload drift impacts the performance of both Bao and Lero, consistent with the trends observed in Figure 7(c).

Discussion: Based on our observations, we summarize the following design trade-offs in learned query optimizers under data and workload drift: 1) Black-box plan search generally achieves better performance than white-box plan search (O1); 2) Cardinality-based plan search demonstrates greater generalizability across different drift scenarios (O2, O4); 3) White-box plan search can be more

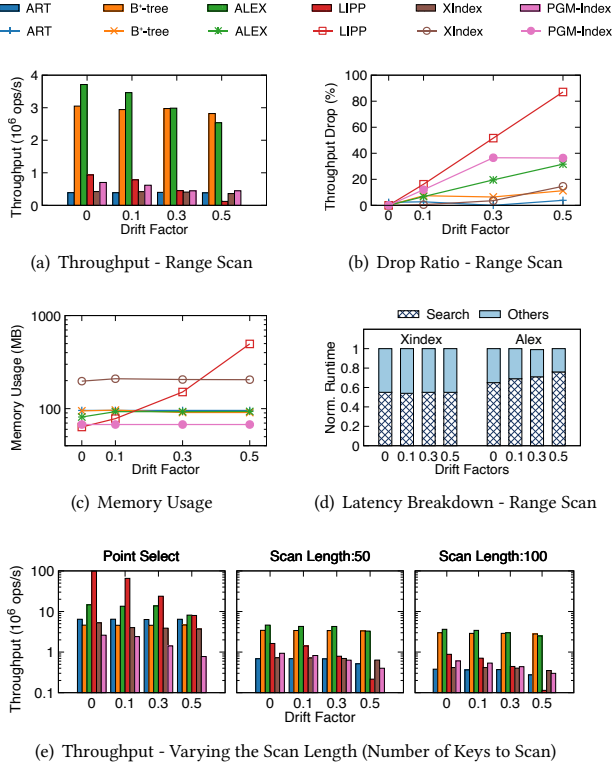


Figure 9: Performance of Learned Indexes under Data Drift with Varying Drift Factors

resilient to data drift than black-box plan search, while top-k plan search enhances generalizability (O3); 4) Join-order-based hints are more susceptible to join pattern drift, whereas general hints provide better adaptability to both join pattern and predicate drift (O5). Given these trade-offs, we envision a more flexible learned query optimizer that dynamically selects the best-performing design choices based on the current system conditions, balancing performance and adaptability under data and workload drift.

6.4 Evaluation on Learned Indexes

We now study the performance of selected learned indexes, *i.e.*, ALEX [13], XIndex [50], PGM-Index [14], and LIPP [60], with varying data drift scenarios. Since all the evaluated learned indexes are in-memory, we include the in-memory implementation of two traditional indexes, Adaptive Radix Tree (ART) [29] and B⁺-tree, as baselines. We use the IMDB Name table, and build the index on the ID attribute as the key and the remaining attributes as values.

6.4.1 Experiments on scan operations, under varying drift factors.

Given a drift factor d , we construct data drift scenarios to evaluate learned index performance, following these steps: 1) Initialize the index on the drifted table generated based on d ; 2) Create a residual set containing records from the original table that are absent in the drifted table; 3) Execute these insert operations to drift the table back toward the original table, and update the index correspondingly. Afterward, we perform range scan operations (specified in Section 6.1.2) on the index with the default settings, unless otherwise specified. All these operations are run with a single thread,

following prior works [13, 60]. We plot the throughput of range scan operations in Figure 9(a) and use Figure 9(b) to show the corresponding throughput drop (defined in Section 6.1.3). We also record the index size after completing the scan operations and present the results in Figure 9(c). We can observe that:

O1: ALEX achieves the highest scan throughput among all evaluated learned indexes across all drift factors. This can be attributed to the heterogeneous structure of ALEX, where data is stored exclusively in the leaf nodes, making its scan process closely resemble that of B⁺-tree. In ALEX, a range scan first locates the position of the start_key by key search, and then sequentially scans the following leaf nodes. In contrast, LIPP employs a homogeneous structure that stores data within each node, preventing it from supporting direct sequential scans. As a result, while ALEX can complete a range scan with a single key search, LIPP requires multiple key searches, leading to higher overhead. Further, although XIndex and PGM-Index also adopt a heterogeneous structure, they maintain separate buffers for handling insertions, which however affects their range scan performance.

O2: The throughput of ALEX and LIPP decreases as drift increases, with LIPP experiencing a more significant drop than ALEX. This is expected because both ALEX and LIPP employ in-place update strategies, which lead to higher key search costs as drift increases, resulting in degraded range scan performance. LIPP in particular, incurs higher key search costs under larger drift because it requires more key searches per range scan than ALEX, as discussed in O1. To further analyze this behavior, we evaluate scan performance under different fixed scan lengths. Specifically, we measure throughput with scan lengths of 1 (point select), 50, and 100, respectively. As shown in Figure 9(e), the throughput of all learned indexes decreases with larger scan length, while LIPP exhibits the steepest drop. Since a larger scan length triggers more key searches, these results confirm that LIPP is more sensitive to key search efficiency.

O3: ALEX incurs a higher performance drop than XIndex with increased drift. These observations indicate that the delta-buffer strategy used in XIndex is more resilient to drift than the in-place update strategy used in ALEX. To verify this, we conduct a latency breakdown analysis for range scan operations. The results in Figure 9(d) demonstrate that for ALEX, key search cost (denoted as “Search”) is the dominant bottleneck, and increases as drift increases. Further, although the scan performance of XIndex can be affected by the additional overhead of buffer scanning (as discussed in O1), this additional cost remains stable due to its fine-grained node-level buffer design, which further contributes to its relatively stable performance under drift.

O4: Only LIPP’s size grows with larger drift, while PGM-Index achieves the smallest index size. LIPP employs an in-place update strategy with a chain method, which splits nodes when conflicts arise in the targeting node. As drift increases, more node splits can potentially occur, causing LIPP’s index size to expand. Retrieving data from a larger index also incurs higher key search costs, which align with our observations in O2. Moreover, PGM-Index maintains a global tree-structured buffer for the entire index, which avoids sparsity and minimizes storage overhead.

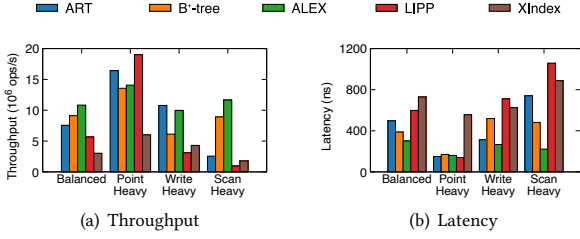


Figure 10: Performance of Learned Indexes with Concurrent Read/Write Access

6.4.2 Experiments on concurrent read/write access under mixed workloads. We evaluate the performance of learned indexes under concurrent read and write workloads. Based on default operations specified in Section 6.1.2, we construct 4 mixed workloads: (1) Balanced workload, which contains 33% inserts to put keys into indexes, 33% point reads to randomly lookup a single key, and 33% range scans to randomly read keys with default scan length. (2) Point-heavy workload, which consists of 90% point reads, 5% writes, and 5% range scans. (3) Write-heavy workload, which contains 90% writes, 5% point reads, and 5% range scans. (4) Scan-heavy workload, which consists of 90% range scans, 5% writes, and 5% point reads. Each experiment executes a total of 4M operations using 4 concurrent threads. We adopt the implementation of ART and B⁺-tree with optimistic lock coupling (OLC) [30] as provided in [55], and use the concurrent implementations of ALEX and LIPP as provided in [59], to conduct our experiments.

We report the throughput and latency across different mixed workloads in Figure 10. We can observe that, under the balanced workload, ALEX outperforms the other indexes due to its relatively stable performance across writes, point reads, and scans. Regarding the point-heavy workload, LIPP archives the best performance because of its precise point-lookup technique. Learned indexes cannot outperform ART under the write-heavy workload, primarily due to their inherent overhead for model updates and maintenance. In addition, ALEX demonstrates superior performance under the scan-heavy workload for similar reasons as discussed in O1.

Discussion: We provide the following design trade-offs in learned indexes under data drift according to our observations: 1) A heterogeneous structure with an in-place insertion strategy achieves the best range scan performance (O1); 2) A heterogeneous structure with a fine-grained delta-buffer strategy can ensure stable range scan performance under drift (O3); 3) A homogeneous structure handles point reads efficiently but cannot perform well for writes and range scans (O2); 4) A tree-level buffer helps minimize index size (O4). Given that the different design choices are suitable for specific drift scenarios and drift-tolerance requirements, we envision that designing a more flexible index structure capable of dynamically adapting to system conditions would be promising.

6.5 Evaluation on Learned Concurrency Control

We now study the throughput of learned Concurrency Control (CC) with varying workload (arrival rate) drift. Our evaluation includes state-of-the-art learned CC, Polyjuice [53], with two traditional CC algorithms, 2PL and OCC [62], and a hybrid CC algorithm, IC3 [54]. We use an initial arrival rate simulated with a single client thread,

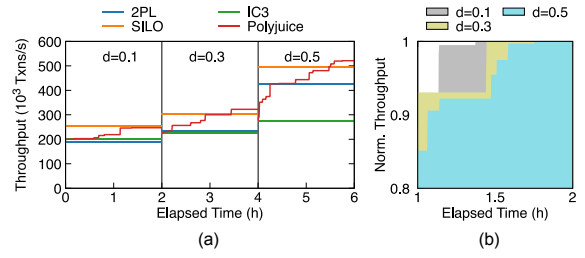


Figure 11: Throughput of Learned CC under Arrival Rate Drift with Varying Drift Factors (Default Workload)

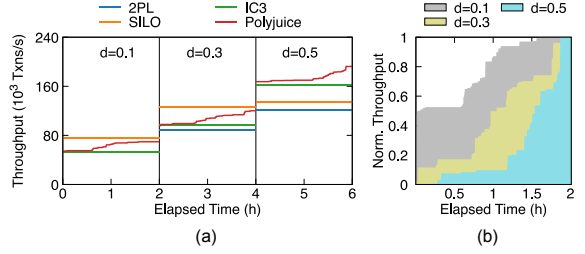


Figure 12: Throughput of Learned CC under Arrival Rate Drift with Varying Drift Factors (CH-Benchmark Workload)

and apply the drift factors from 0.1 to 0.5, which gradually increases transaction arrival rates. Polyjuice is first trained on the initial arrival rate and then retrained after each arrival rate drift, following the retraining procedure outlined in [53]. We perform the default transactions specified in Section 6.1.2. Figure 11(a) plots the transaction throughput, while Figure 11(b) presents the corresponding normalized throughput. The results show that, as drift increases, Polyjuice achieves higher throughput due to the increased arrival rate. However, Polyjuice requires more time for convergence to the most efficient policy under higher drift. This can be attributed to the fact that greater drift increases the complexity of learning an optimal policy due to limited prior knowledge. In addition, Polyjuice’s retraining process is time-consuming, which hinders its ability to adapt efficiently to continuous arrival rate drift.

We conduct additional experiments using the CH-Benchmark workload under transaction arrival rate drift. Specifically, we run our evaluations on the transactional workloads from CH-Benchmark with varying the drift factor across 0.1, 0.3, and 0.5. The transaction throughput results are presented in Figure 12. As shown in the figure and consistent with observations in Figure 11, Polyjuice achieves higher throughput but requires longer convergence time to reach an optimal policy as the drift factor increases.

Discussion: A learned CC algorithm must understand transactional dependencies and actions to be taken when conflicts arise in its learning. Fast adaptation is crucial for learned CC to be practical in real-world scenarios since transactions can be completed in milliseconds or less. To validate this point, we perform additional experiments to assess CCaLF [44], a recently proposed learned CC algorithm that enables fast adaptation under dynamic workloads. We rerun our experiments on both the default workloads and CH-Benchmark workloads under arrival rate drift ($d = 0.5$), and plot the results in Figure 13. As observed, CaaLF achieves higher throughput and faster convergence than Polyjuice. This improved adaptability

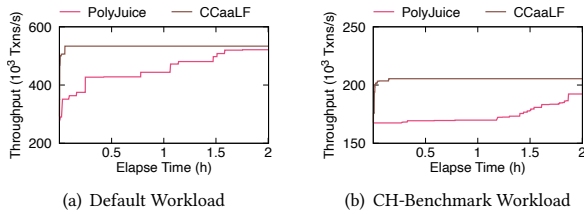


Figure 13: CCaaLF vs PolyJuice (Arrival Rate Drift with Drift Factor $d=0.5$)

is mainly due to the fact that CCaaLF explicitly models transaction dependencies in action selection, enabling it to dynamically adjust its policy based on the current system state.

7 RELATED WORK

Benchmarks for Learned Database Components. Multiple benchmarks have been devised for various learned database components, such as learned query optimizers [6, 18], learned indexes [26, 48], disk-oriented [26, 37] and hardware-enhanced learned components [41, 65], etc. Recent studies [39, 67] also attempt to explore benchmarking learned database components under drifted data or workloads. However, their drift modeling remains simplistic, failing to capture diverse drift scenarios needed for a systematic performance assessment across different learned database components. NeurBench, in contrast, provides controllable and effective drifted data and workload generation, enabling a more comprehensive performance evaluation under diverse drift scenarios.

Benchmarks with Distribution Drift. Several benchmarks have been developed to evaluate performance under distribution drift. DSB [12] a standard benchmark for decision-making applications, enables evaluations under distribution drift using TPC-DS. However, it is restricted to exponential distributions and cannot quantitatively measure drift as NeurBench. Concept drift modeling [4, 33, 45] has gained traction in ML-related fields. However, they are not directly applicable to database benchmarking, as they either focus on non-tabular data or fail to consider the various types of drift that occur in databases. Emerging dynamic benchmarks [3] show promising potential. As a dynamic benchmark, NeurBench introduces measurable and controllable data and workload drift based on real drifts to enable systematic performance evaluations.

8 CONCLUSIONS

This paper introduced NeurBench, a new benchmark suite designed to evaluate end-to-end learned DBMSs containing all learned components under controllable data and workload drift. We defined the drift factor to effectively quantify drift, and introduce a novel drift-aware data and workload generation framework. Extensive experimental results show the effectiveness of NeurBench in drifted data and workload generation, and demonstrate that different learned database components withstand and adapt to data and workload drift to varying degrees, depending on their specific design choices. Through in-depth analysis, we offer recommendations for enhancing the adaptability of learned database components.

REFERENCES

[1] Christoph Anneser, Nesime Tatbul, David E. Cohen, Zhenggang Xu, Prithviraj Pandian, Nikolay Laptev, and Ryan Marcus. 2023. AutoSteer: Learned Query Optimization for Any SQL Database. *Proc. VLDB Endow.* 16, 12 (2023), 3515–3527.

[2] Internet Archive. 2025. *IMDB Archive*. <https://web.archive.org/web/20240301000000/https://datasets.imdbws.com/>

[3] Lawrence Benson, Carsten Binnig, Jan-Micha Bodensohn, Federico Lorenzi, Jigao Luo, Danica Porobic, Tilmann Rabl, Anupam Sanghi, Russell Sears, Pinar Tözün, and Tobias Ziegler. 2024. Surprise Benchmarking: The Why, What, and How. In *DBTest@SIGMOD*. ACM, 1–8.

[4] Maximilian Böther, Foteini Strati, Viktor Gsteiger, and Ana Klimovic. 2023. Towards A Platform and Benchmark Suite for Model Training on Dynamic Datasets. In *EuroMLSys@EuroSys*. ACM, 8–17.

[5] Tianyi Chen, Jun Gao, Hedui Chen, and Yaofeng Tu. 2023. LOGER: A Learned Optimizer towards Generating Efficient and Robust Query Execution Plans. *Proc. VLDB Endow.* 16, 7 (2023), 1777–1789.

[6] Yannis Chronis, Yawen Wang, Yu Gan, Sami Abu-El-Haija, Chelsea Lin, Carsten Binnig, and Fatma Özcan. 2024. CardBench: A Benchmark for Learned Cardinality Estimation in Relational Databases. *CoRR* abs/2408.16170 (2024).

[7] Prafulla Cole, Florian Funke, Leo Giakoumakis, Wey Guy, Alfons Kemper, Stefan Krompass, Harumi Kuno, Raghunath Nambiar, Thomas Neumann, Meikel Poess, et al. 2011. The mixed workload CH-benCHmark. In *Proceedings of the Fourth International Workshop on Testing Database Systems*. 1–6.

[8] Brian F. Cooper, Adam Silberstein, Erwin Tam, Raghu Ramakrishnan, and Russell Sears. 2010. Benchmarking cloud serving systems with YCSB. In *SoCC*. ACM, 143–154.

[9] The Transaction Processing Council. 2024. *TPC-C*. <http://www.tpc.org/tpcc/>

[10] The Transaction Processing Council. 2024. *TPC-H*. <http://www.tpc.org/tpch/>

[11] Prafulla Dhariwal and Alexander Quinn Nichol. 2021. Diffusion Models Beat GANs on Image Synthesis. In *NeurIPS*. 8780–8794.

[12] Bailu Ding, Surajit Chaudhuri, Johannes Gehrke, and Vivek R. Narasayya. 2021. DSB: A Decision Support Benchmark for Workload-Driven and Traditional Database Systems. *Proc. VLDB Endow.* 14, 13 (2021), 3376–3388.

[13] Jialin Ding, Umar Farooq Minhas, Jia Yu, Chi Wang, Jaeyoung Do, Yanan Li, Hantian Zhang, Badrish Chandramouli, Johannes Gehrke, Donald Kossmann, David B. Lomet, and Tim Kraska. 2020. ALEX: An Updatable Adaptive Learned Index. In *SIGMOD Conference*. ACM, 969–984.

[14] Paolo Ferragina and Giorgio Vinciguerra. 2020. The PGM-index: a fully-dynamic compressed learned index with provable worst-case bounds. *Proc. VLDB Endow.* 13, 8 (2020), 1162–1175.

[15] Josh Gardner, Zoran Popovic, and Ludwig Schmidt. 2023. Benchmarking Distribution Shift in Tabular Data with TableShift. In *NeurIPS*.

[16] Minas Gjoka, Maciej Kurant, Carter T. Butts, and Athina Markopoulou. 2010. Walking in Facebook: A Case Study of Unbiased Sampling of OSNs. In *INFOCOM*. IEEE, 2498–2506.

[17] Zhihan Guo, Kan Wu, Cong Yan, and Xiangyao Yu. 2021. Releasing Locks As Early As You Can: Reducing Contention of Hotspots by Violating Two-Phase Locking. In *SIGMOD Conference*. ACM, 658–670.

[18] Yuxing Han, Ziniu Wu, Peizhi Wu, Rong Zhu, Jingyi Yang, Liang Wei Tan, Kai Zeng, Gao Cong, Yanzhao Qin, Andreas Pfadler, Zhengping Qian, Jingren Zhou, Jiangneng Li, and Bin Cui. 2021. Cardinality Estimation in DBMS: A Comprehensive Benchmark Evaluation. *Proc. VLDB Endow.* 15, 4 (2021), 752–765.

[19] Jonathan Ho, Ajay Jain, and Pieter Abbeel. 2020. Denoising Diffusion Probabilistic Models. In *NeurIPS*.

[20] IMDB. 2025. *IMDB Dataset*. <https://www.imdb.com/>

[21] Pang Wei Koh, Shiori Sagawa, Henrik Marklund, Sang Michael Xie, Marvin Zhang, Akshay Balsubramani, Weihua Hu, Michihiro Yasunaga, Richard Lanus Phillips, Irena Gao, Tony Lee, Etienne David, Ian Stavness, Wei Guo, Berton Earnshaw, Imran S. Haque, Sara M. Beery, Jure Leskovec, Anshul Kundaje, Emma Pierson, Sergey Levine, Chelsea Finn, and Percy Liang. 2021. WILDS: A Benchmark of in-the-Wild Distribution Shifts. In *ICML (Proceedings of Machine Learning Research, Vol. 139)*. PMLR, 5637–5664.

[22] Akim Kotelnikov, Dmitry Baranchuk, Ivan Rubachev, and Artem Babenko. 2023. TabDDPM: Modelling Tabular Data with Diffusion Models. In *ICML (Proceedings of Machine Learning Research, Vol. 202)*. PMLR, 17564–17579.

[23] Tim Kraska, Alex Beutel, Ed H. Chi, Jeffrey Dean, and Neoklis Polyzotis. 2018. The Case for Learned Index Structures. In *SIGMOD Conference*. ACM, 489–504.

[24] Meghdad Kurmanji, Eleni Triantafillou, and Peter Triantafillou. 2024. Machine Unlearning in Learned Databases: An Experimental Analysis. *Proc. ACM Manag. Data* 2, 1 (2024), 49:1–49:26.

[25] Meghdad Kurmanji and Peter Triantafillou. 2023. Detect, Distill and Update: Learned DB Systems Facing Out of Distribution Data. *Proc. ACM Manag. Data* 1, 1 (2023), 33:1–33:27.

[26] Hai Lan, Zhifeng Bao, J. Shane Culpepper, and Renata Borovica-Gajic. 2023. Updatable Learned Indexes Meet Disk-Resident DBMS - From Evaluations to Design Choices. *Proc. ACM Manag. Data* 1, 2 (2023), 139:1–139:22.

[27] Claude Lehmann, Pavel Sulimov, and Kurt Stockinger. 2024. Is Your Learned Query Optimizer Behaving As You Expect? A Machine Learning Perspective. *Proc. VLDB Endow.* 17, 7 (2024), 1565–1577.

- [28] Viktor Leis, Andrey Gubichev, Atanas Mirchev, Peter A. Boncz, Alfons Kemper, and Thomas Neumann. 2015. How Good Are Query Optimizers, Really? *Proc. VLDB Endow.* 9, 3 (2015), 204–215.
- [29] Viktor Leis, Alfons Kemper, and Thomas Neumann. 2013. The adaptive radix tree: ARTful indexing for main-memory databases. In *ICDE*. IEEE Computer Society, 38–49.
- [30] Viktor Leis, Florian Scheibner, Alfons Kemper, and Thomas Neumann. 2016. The ART of practical synchronization. In *DaMoN*. ACM, 3:1–3:8.
- [31] Beibin Li, Yao Lu, and Srikanth Kandula. 2022. Warper: Efficiently Adapting Learned Cardinality Estimators to Data and Workload Drifts. In *SIGMOD Conference*. ACM, 1920–1933.
- [32] Pengfei Li, Wenqing Wei, Rong Zhu, Bolin Ding, Jingren Zhou, and Hua Lu. 2023. ALECE: An Attention-based Learned Cardinality Estimator for SPJ Queries on Dynamic Workloads. *Proc. VLDB Endow.* 17, 2 (2023), 197–210.
- [33] Wendi Li, Xiao Yang, Weiqing Liu, Yingce Xia, and Jiang Bian. 2022. DDG-DA: Data Distribution Generation for Predictable Concept Drift Adaptation. In *AAAI Press*, 4092–4100.
- [34] Yu-Shan Lin, Ching Tsai, Tz-Yu Lin, Yun-Sheng Chang, and Shan-Hung Wu. 2021. Don't Look Back, Look into the Future: Prescient Data Partitioning and Migration for Deterministic Database Systems. In *SIGMOD Conference*. ACM, 1156–1168.
- [35] Haohe Liu, Zehua Chen, Yi Yuan, Xinhao Mei, Xubo Liu, Danilo P. Mandic, Wenwu Wang, and Mark D. Plumbley. 2023. AudioLDM: Text-to-Audio Generation with Latent Diffusion Models. In *ICML (Proceedings of Machine Learning Research, Vol. 202)*. PMLR, 21450–21474.
- [36] Tongyu Liu, Ju Fan, Nan Tang, Guoliang Li, and Xiaoyong Du. 2024. Controllable Tabular Data Synthesis Using Diffusion Models. *Proc. ACM Manag. Data* 2, 1 (2024), 28:1–28:29.
- [37] Chaohong Ma, Xiaohui Yu, Yifan Li, Xiaofeng Meng, and Aishan Maoliniaz. 2022. FILM: a Fully Learned Index for Larger-than-Memory Databases. *Proc. VLDB Endow.* 16, 3 (2022), 561–573.
- [38] Christopher D. Manning and Hinrich Schütze. 2001. *Foundations of statistical natural language processing*. MIT Press.
- [39] Ryan Marcus, Parimarjan Negi, Hongzi Mao, Nesime Tatbul, Mohammad Alizadeh, and Tim Kraska. 2021. Bao: Making Learned Query Optimization Practical. In *SIGMOD Conference*. ACM, 1275–1288.
- [40] Ryan Marcus, Parimarjan Negi, Hongzi Mao, Chi Zhang, Mohammad Alizadeh, Tim Kraska, Olga Papaemmanouil, and Nesime Tatbul. 2019. Neo: A Learned Query Optimizer. *Proc. VLDB Endow.* 12, 11 (2019), 1705–1718.
- [41] Songsong Mo, Yile Chen, Hao Wang, Gao Cong, and Zhifeng Bao. 2023. Lemo: A Cache-Enhanced Learned Optimizer for Concurrent Queries. *Proc. ACM Manag. Data* 1, 4 (2023), 247:1–247:26.
- [42] Lili Mou, Ge Li, Lu Zhang, Tao Wang, and Zhi Jin. 2016. Convolutional Neural Networks over Tree Structures for Programming Language Processing. In *AAAI AAAI Press*, 1287–1293.
- [43] NeurBench. 2025. *NeurBench Implementation*. <https://github.com/neurdb/neurbench>
- [44] Hexiang Pan, Shaofeng Cai, Yeow Meng Chee, Tien Tuan Anh Dinh, Yuncheng Wu, and Beng Chin Ooi. 2025. CCaaLF: Concurrency Control as a Learnable Function. *CoRR abs/2503.10036* (2025).
- [45] Piotr Porwik and Benjamin Mensah Dadzie. 2022. Detection of data drift in a two-dimensional stream using the Kolmogorov-Smirnov test. In *KES (Procedia Computer Science, Vol. 207)*. Elsevier, 168–175.
- [46] Cemal Okan Sakar, Suleyman Olcay Polat, Mete Katircioglu, and Yomi Kastro. 2019. Real-time prediction of online shoppers' purchasing intention using multi-layer perceptron and LSTM recurrent neural networks. *Neural Comput. Appl.* 31, 10 (2019), 6893–6908.
- [47] Jascha Sohl-Dickstein, Eric A. Weiss, Niru Maheswaranathan, and Surya Ganguli. 2015. Deep Unsupervised Learning using Nonequilibrium Thermodynamics. In *Proceedings of the 32nd International Conference on Machine Learning, ICML 2015, Lille, France, 6–11 July 2015 (JMLR Workshop and Conference Proceedings, Vol. 37)*, Francis R. Bach and David M. Blei (Eds.). JMLR.org, 2256–2265.
- [48] Zhaoyan Sun, Xuanhe Zhou, and Guoliang Li. 2023. Learned Index: A Comprehensive Experimental Evaluation. *Proc. VLDB Endow.* 16, 8 (2023), 1992–2004.
- [49] Kai Sheng Tai, Richard Socher, and Christopher D. Manning. 2015. Improved Semantic Representations From Tree-Structured Long Short-Term Memory Networks. In *ACL (1)*. The Association for Computer Linguistics, 1556–1566.
- [50] Chuzhe Tang, Youyun Wang, Zhiyuan Dong, Gansen Hu, Zhaoguo Wang, Minjie Wang, and Haibo Chen. 2020. XIndex: a scalable learned index for multicore data storage. In *PPoPP*. ACM, 308–320.
- [51] Dixin Tang, Hao Jiang, and Aaron J. Elmore. 2017. Adaptive Concurrency Control: Despite the Looking Glass, One Concurrency Control Does Not Fit All. In *CIDR*. www.cidrdb.org.
- [52] Ashish Vaswani, Noam Shazeer, Niki Parmar, Jakob Uszkoreit, Llion Jones, Aidan N. Gomez, Lukasz Kaiser, and Illia Polosukhin. 2017. Attention is All you Need. In *NIPS*. 5998–6008.
- [53] Jia-Chen Wang, Ding Ding, Huan Wang, Conrad Christensen, Zhaoguo Wang, Haibo Chen, and Jinyang Li. 2021. Polyjuice: High-Performance Transactions via Learned Concurrency Control. In *OSDI*. USENIX Association, 198–216.
- [54] Zhaoguo Wang, Shuai Mu, Yang Cui, Han Yi, Haibo Chen, and Jinyang Li. 2016. Scaling Multicore Databases via Constrained Parallel Execution. In *SIGMOD Conference*. ACM, 1643–1658.
- [55] Ziqi Wang, Andrew Pavlo, Hyeontaek Lim, Viktor Leis, Huanchen Zhang, Michael Kaminsky, and David G. Andersen. 2018. Building a Bw-Tree Takes More Than Just Buzz Words. In *SIGMOD Conference*. ACM, 473–488.
- [56] WeatherAUS. 2025. *WeatherAUS DataSet*. <https://www.kaggle.com/jsphyy/weather-dataset-rattle-package>
- [57] Wikipedia. 2025. *Pearson Correlation Coefficient*. https://en.wikipedia.org/wiki/Pearson_correlation_coefficient
- [58] Olivia Wiles, Sven Gowal, Florian Stimberg, Sylvestre-Alvise Rebuffi, Ira Ktena, Krishnamurthy Dvijotham, and Ali Taylan Cemgil. 2022. A Fine-Grained Analysis on Distribution Shift. In *ICLR*. OpenReview.net.
- [59] Chaichon Wongkham, Baotong Lu, Chris Liu, Zhicong Zhong, Eric Lo, and Tianzheng Wang. 2022. Are Updatable Learned Indexes Ready? *Proc. VLDB Endow.* 15, 11 (2022), 3004–3017.
- [60] Jiacheng Wu, Yong Zhang, Shimin Chen, Yu Chen, Jin Wang, and Chunxiao Xing. 2021. Updatable Learned Index with Precise Positions. *Proc. VLDB Endow.* 14, 8 (2021), 1276–1288.
- [61] Peizhi Wu and Zachary G. Ives. 2024. Modeling Shifting Workloads for Learned Database Systems. *Proc. ACM Manag. Data* 2, 1 (2024), 38:1–38:27.
- [62] Yu Xia, Xiangyao Yu, Matthew Butrovich, Andrew Pavlo, and Srinivas Devadas. 2022. Litmus: Towards a Practical Database Management System with Verifiable ACID Properties and Transaction Correctness. In *SIGMOD Conference*. ACM, 1478–1492.
- [63] Xiang Yu, Chengliang Chai, Guoliang Li, and Jiabin Liu. 2022. Cost-based or Learning-based? A Hybrid Query Optimizer for Query Plan Selection. *Proc. VLDB Endow.* 15, 13 (2022), 3924–3936.
- [64] Shunkang Zhang, Ji Qi, Xin Yao, and André Brinkmann. 2024. Hyper: A High-Performance and Memory-Efficient Learned Index via Hybrid Construction. *Proc. ACM Manag. Data* 2, 3 (2024), 145.
- [65] Zhou Zhang, Zhaole Chu, Peiquan Jin, Yongping Luo, Xike Xie, Shouhong Wan, Yun Luo, Xufei Wu, Peng Zou, Chunyang Zheng, Guoan Wu, and Andy Rudoff. 2022. PLIN: A Persistent Learned Index for Non-Volatile Memory with High Performance and Instant Recovery. *Proc. VLDB Endow.* 16, 2 (2022), 243–255.
- [66] Rong Zhu, Wei Chen, Bolin Ding, Xingguang Chen, Andreas Pfadler, Ziniu Wu, and Jingren Zhou. 2023. Lero: A Learning-to-Rank Query Optimizer. *Proc. VLDB Endow.* 16, 6 (2023), 1466–1479.
- [67] Rong Zhu, Liangui Weng, Bolin Ding, and Jingren Zhou. 2024. Learned Query Optimizer: What is New and What is Next. In *SIGMOD Conference Companion*. ACM, 561–569.